ORIGINAL ARTICLE

FGM based on copper–alumina composites for brake disc applications

Agata Strojny-Nędza[1] · Katarzyna Pietrzak[1,2] · Flavia Gili[3] · Marcin Chmielewski[1]

Abstract

Copper–alumina composites of the interpenetrating networks type are interesting materials for many applications because of their properties. On the base of preliminary investigations and practical works, in order to obtain a material with high resistance to friction wear as well as good dissipation of heat generated during work, it was decided that a developed material would be prepared on the base of the $Cu–Al_2O_3$ composite, with a graded composition. In this paper, we present the developed method of manufacturing dense copper–alumina FGMs, using ceramic preform with a graded porosity infiltrated with molten copper. The article also presents the full characterization of the obtained materials and mainly the impact of microstructure on the useful properties. The produced gradient material of a $Cu–Al_2O_3$ brake disk underwent tribological tests under conditions resembling real conditions. These disks also went through a series of abrasive wear trials at different operation stages. In comparison with the reference material (i.e., grey cast iron), the obtained gradient materials are characterized by a lower degree of wear when retaining a similar coefficient of friction value due to the ceramic phase addition. Additionally, it was found that using the copper-based gradient material guarantees faster heat dissipation from the contact area.

Keywords Composites · Interpenetrating network materials · Functionally gradient materials · Brake disc

1 Introduction

Metal–ceramic composites have been widely applied in industries, like aerospace, automotive, and in many others [1]. In [2], this is explained by their high ratio of strength to mass and specific stiffness as well as excellent thermal conductivity and excellent wear resistance. The automotive industry needs improvement related not only to improved driving comfort and safety, but also to increased efficiency of fuel consumption and emission standards, which translates into a reduction in the weight of vehicles by using such composites [3]. Therefore, it seems that an important aspect is the improvement in wear resistance at elevated temperatures as well as the improvement in mechanical properties. Wannasin [4] suggests that interesting material solution is interpenetration network composites (IPCs). Composites with a high ceramic phase content are usually obtained by infiltration (under pressure or non-pressure) of porous ceramic preforms with liquid metal. In [5], it was reported that composites of the type of interpenetrating phases of ceramics and metal IPCs with given functionality (e.g., high thermal conductivity) and increased bending strength, resistance to cracking and abrasion as well as resistance to temperature are interested. In [6] the authors obtained Al_2O_3–Cu composites by infiltration of porous preforms by copper and, based on tests of their properties, stated that these materials have very good thermal, electric, and mechanical properties. The materials used in brake rotors should absorb and dissipate the heat generated during braking. Therefore, when designing brake discs, it is very important to prevent excessive temperature increase in its working elements. Ceramic and metal composite materials are characterized by high resistance to thermal shocks, necessary, for example, when the brake disk contacts the water [7]. In another work [8], it is confirmed that good mechanical and tribological properties provide the properties of ceramics and the addition of metal raises, among others, the value of thermal conductivity
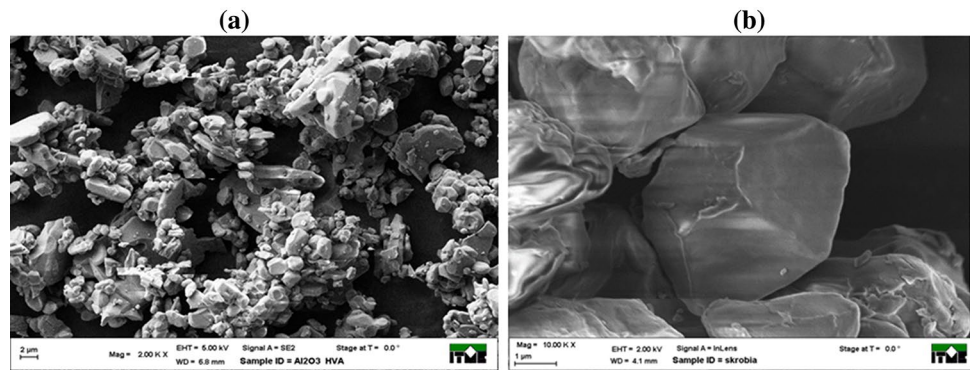
✉ Agata Strojny-Nędza
  agata.strojny@itme.edu.pl

1 Research Network ŁUKASIEWICZ, Institute of Electronic Materials Technology, 133 Wólczyńska Str., 01-919 Warsaw, Poland

2 Institute of Fundamental Technological Research, Polish Academy of Sciences, 5A Pawinskiego Str., 02-106 Warsaw, Poland

3 CRF, Centro Ricerche Fiat, Strada Torino 50, Orbassano, Italy

Fig. 1 SEM micrograph of alumina powder (**a**) and rice starch powder (**b**)

and increases resistance to cracking. Sobczak suggests that composite brake discs could potentially have a longer lifetime and also be lighter than the typical grey iron disc, an important feature for reducing fuel consumption [9]. Reinforced aluminum composites have been introduced as disc materials [10, 11]. The developed technology of manufacturing interpenetrating phase composites as well as composites with a composition gradient offers ample opportunities of their application in solutions where the main factor is wear as well as heat generation in working conditions [12, 13]. An increased resistant to abrasive wear, in addition to increasing the material's life span, also influences the elimination of the possibility of occurrence of toxic wear products that pollute the natural environment [14]. The main point of this work was to develop a gradient material Cu–Al$_2$O$_3$ with interpenetrating network structure in view of potential application of these composites in the automotive industry. The purpose of the proposed structure of a gradient composite was to maximally reduce local tensile stress in the ceramic phase and on the metal/ceramic phase boundary that occurs inside FGM layer, while at the same time obtaining high values of technical parameters resulting from the combination of the properties of metal and ceramics. The developed technology of FGM material manufacture was also to ensure material stability in heightened and variable temperature, as well as a stable friction coefficient in conditions similar to real conditions (conditions similar to those of a working brake disc).

2 Experimental procedure

2.1 Preparation of ceramic slurry and porous preform

Ceramic porous preforms were fabricated using the tape casting technique. Commercially available αAl$_2$O$_3$ powder (Almatis, grain size 4.8 μm) was used to prepare slurry mixture and next ceramic green bodies as individual foil and compacted preform (Fig. 1a). The ceramic slurry, consisted of aluminum oxide powder, binder, plasticizer, surfactant,
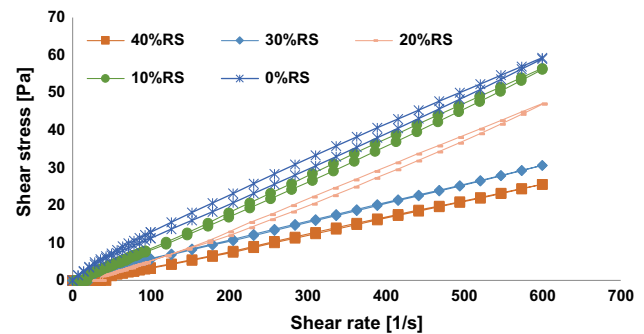

Fig. 2 Rheology of ceramic slurry for the different composition

Table 1 The values of dynamic viscosity of slip masses at a shear rate of 100 1/s

	0% RS	10% RS	20% RS	30% RS	40% RS
Dynamic viscosity (Pa/s)	0.113	0.083	0.058	0.055	0.034

and pore-forming agent, was mixed using ball mill. The rice starch (RS) powder (Remy, grain size 5.0 μm) was used as a pore-forming agent (Fig. 1b). The mixing process was conducted at RT in air using rotational speed 300 rpm, mixing time 90 min, and BPR 3:1.

The quantitative and qualitative composition of the slurries needed for the preparation of ceramic foils was selected based on the results of research on their rheological properties and on the basis of macroscopic observation of the obtained foils. The obtained results of the shear stress dependence on shear rate showed that the slurries possess a small hysteresis loop and thus low values of the thixotropy coefficient, which indicates their stability over time (Fig. 2).

The obtained values of dynamic viscosity for various compositions of slip masses for a shear rate of 100 1/s are presented in Table 1.

The viscosity of the slurry is significantly impacted by the concentration of the solid phase; the higher the

concentration, the higher the viscosity [15]. With the addition of rice starch, the amount of the liquid phase added to the mass (in order to liquify it) increases, and thereby the concentration of the solid state decreases. Another very important factor impacting the viscosity value is the distribution of particle size in the slurry. The viscosity of the slurry, where an appropriate fraction of smaller particles is present alongside larger particles (polydisperse slurry), is lower than when powder is used that consists of large, uniform particles (monodisperse slurry).The doctor blade technique [16, 17] was used to ceramic foil casting preparation process. The obtained foils were dried for 24 h at the room temperature and finally removed from the surface of the belt. The thickness of the foils was in the range of 0.2–0.3 mm. Finally, the ceramic foils were cut and stacked to prepare gradient preforms with different amounts of rice starch. Then, a lamination process was conducted using an external pressure of 40 MPa at the temperature of 100 °C in a metal form. Four-layered gradient preform (FGM), consisted of over forty individual foils, was prepared, as shown in Fig. 3. It was assumed that the first and last layers would form the thickest layers in the FGM material. Such a selection of the composition of the gradient material is the result of its intended function. When selecting the composition of a gradient material, achieving the planned goals was the principle followed. The material prepared for a brake disc demonstrator was to fulfill two basic functions above all, i.e., to be resistant to abrasive wear (the inner side of the disc should contain a larger amount of the ceramic phase) as well as to dissipate heat efficiently that would be generated while the disc is working (the outer side of the disc with a higher volume fraction of copper, characterizing by high thermal conductivity). As a reference sample, an un-graded demonstrator preform (UD) that consisted of 40% RS foils was prepared.

The sintering process of ceramic preforms was divided into two stages [18]. The organic additives' burnt-out process was conducted at a temperature of 1100 °C with the intermediate stop at temperature 600 °C. The heating rate was as follows: 0.8 °C/min for RT–600 °C and 2.0 °C/min for 600–1100 °C heating range. It was assumed that minimum open porosity in the ceramic preforms to be infiltrated with liquid metal should be 30%. This is a critical value of material porosity a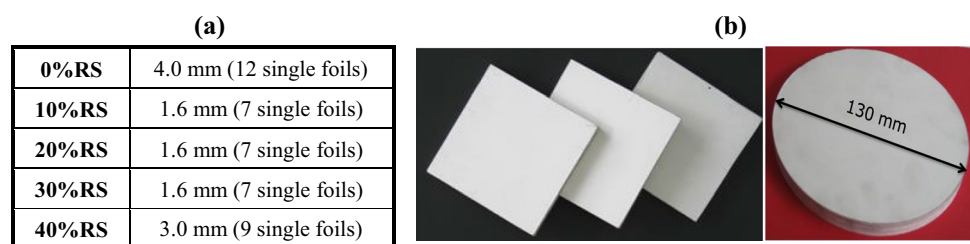t which infiltration may occur (the classic problem in percolation theory). This is related to the occurrence of an infinite cluster, i.e., a channel (with complicated geometry) from one side of the sample to the other [19]. The targeted porosity (30%) in the ceramic preforms was obtained at the sintering temperature of 1670 °C and 60 min sintering time. During the organic component burnout, open channels of pores were created. It was found that the ceramic preform porosity is higher than the added amount of pore agent (rice starch) due to inherent pores present in the ceramic. Consequently, all of the FGM layers had some additional porosity that contributed to the total porosity.

2.2 Fabrication process of Cu–Al$_2$O$_3$ composites and FGM Cu–Al$_2$O$_3$

Fabrication process based on infiltration technique was made at Institute of Materials and Machines of Slovak Academy of Science (IMSAS) in Bratislava, Slovakia. The squeeze casting process of the graded and ungraded preforms with molten copper was conducted at 1280 °C using 10 MPa pressure for 90 s. Before the infiltration process, porous preforms were preheated to about 700 °C. The turbulent filling process may cause the formation of copper oxides film, which can negatively influence on the composite properties. The process conditions should limit the possibility of cracks forming in the ceramic preform because of thermal shock. In the first stage of the copper infiltration process, the threshold capillary resistance of the porous ceramic has to be overcome by the pressure used. Next, the infiltration process occurs in a stable way until the open pores in the ceramic structure are fully filled up. Photographs of infiltrated demonstrators of a brake disc are shown in Fig. 4. Additionally, for basic materials properties measurements the non-graded composite materials were performed. Cu–Al$_2$O$_3$ composites with a different volume fraction of the ceramic phase in the range of 30–50 vol% were prepared.

When liquid metal is poured into a ceramic preform, it is subject to forces that cause high tensions in the preform. The proper mechanical strength of the preform ensures that it keeps its initial shape in the process of pressure infiltration. It is therefore crucial to manufacture porous materials that can withstand the forces acting upon them during infiltration so that no microcracks occur in the volume of the material (preform) that could result in breakage

Fig. 3 The composition of graded samples for a demonstrator brake disk (**a**) and laminated samples (**b**)
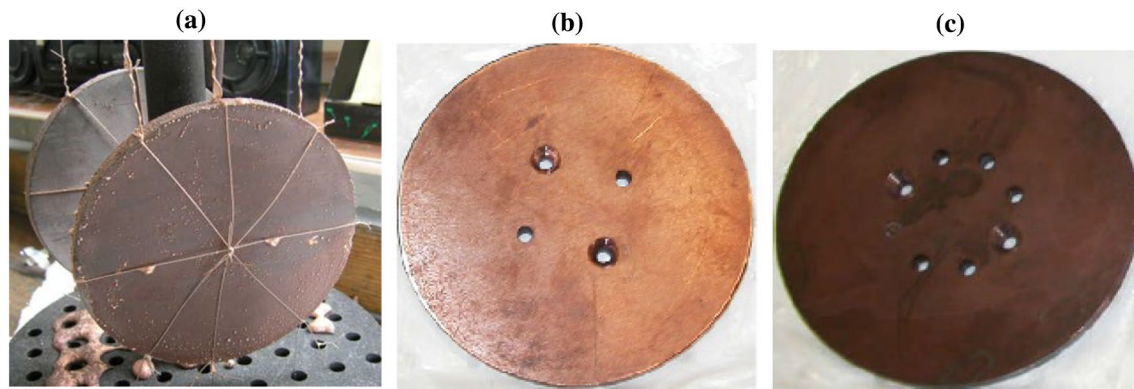
(a)	
0%RS	4.0 mm (12 single foils)
10%RS	1.6 mm (7 single foils)
20%RS	1.6 mm (7 single foils)
30%RS	1.6 mm (7 single foils)
40%RS	3.0 mm (9 single foils)

Fig. 4 Photograph of infiltrated copper–alumina demonstrator (**a**): gradient (FGMD) (**b**) and un-gradient (UD) (**c**)

and therefore destruction during the exploitation of the material. The applied parameters of the process ensured complete infiltration of the ceramic preforms, and no destruction of ceramic preforms during the process was observed.

2.3 Microstructure, mechanical, and thermal analysis methods

The microstructures of materials were examined using AURIGA CrossBeam Workstation SEM. The Vickers hardness (HV5) measurements were performed with a diamond indenter using DuraScan-20 Struers apparatus. ZWICK 1446 testing machine was used to determine the bending strength of the composites. The test was made in a three-point bending mode, the displacement speed of 1 mm/min, and the head load of 10 kN. LFA457/Netzsch was used to estimate the thermal conductivity.

2.4 Application tests

The prepared demonstrators of a brake disc (gradient (FGMD) as well as un-gradient (UD) underwent tests of tribological properties in CRF in Turin. Application tests were conducted that consisted in testing the friction wear resistance of the prepared demonstrators. Steel with copper and zirconium additives was used as the material of the counter-sample. Wear tests of the disc brake demonstrators were conducted in various conditions (tests under application near conditions). In the first work cycle, varying loads were adopted with a constant rotation speed of the disc in dry lubrication conditions; in the second cycle, water was used as the lubricant for wet lubrication conditions; in the last cycle, changing conditions were adopted, i.e., changing rotation speed of the disc and varying pressure (Fig. 5).

3 Results and discussion

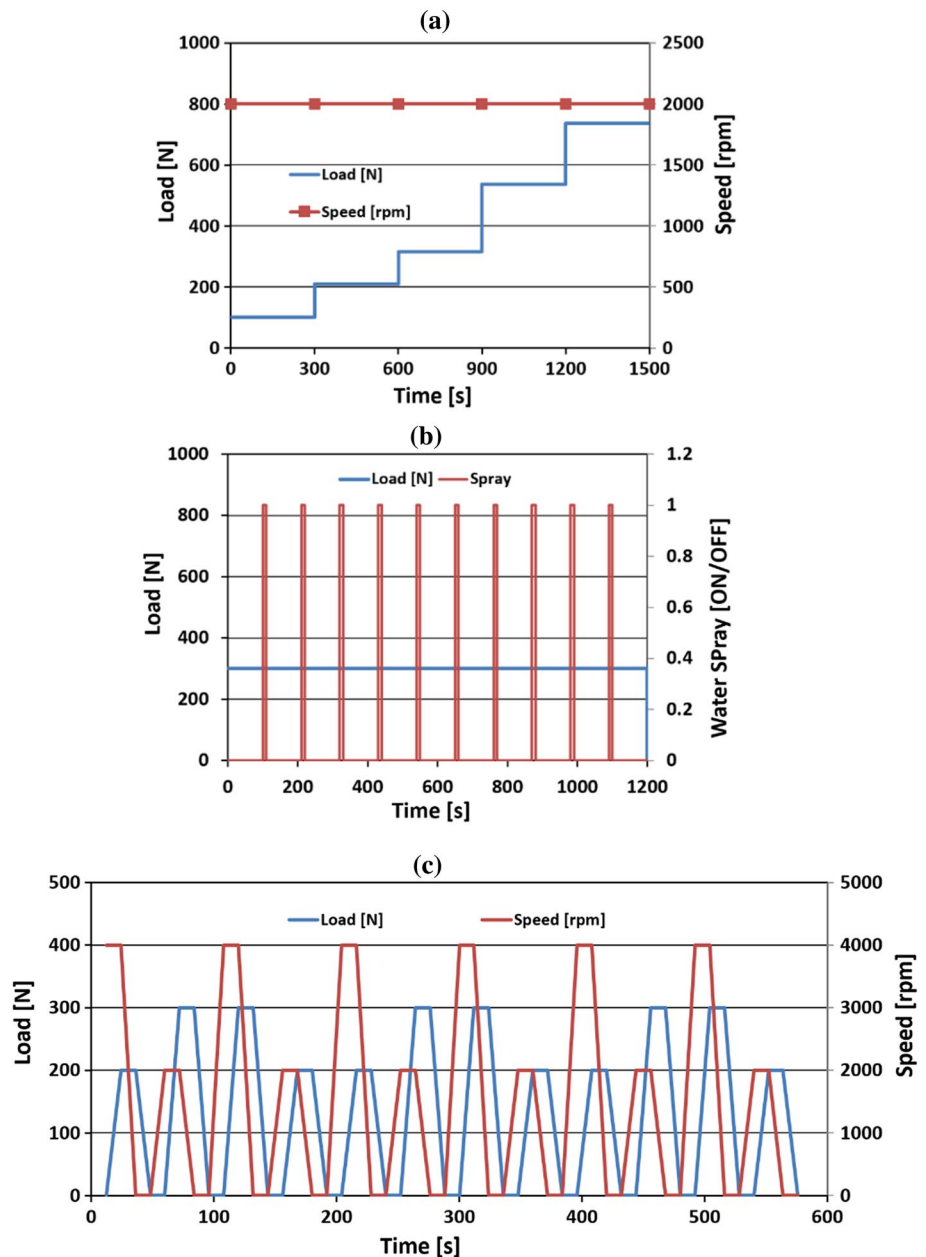### 3.1 Characterization of ceramic, porous preforms

The obtained porous ceramic preforms were subjected to characterization of their physical and mechanical properties. In order to determine the porosity of ceramic preforms, pore size distribution tests were performed on a porosimeter (Fig. 6). In addition, porosity measurements were made via the Clemex television image analysis method. The obtained results of porosity and average pore sizes in ceramic preforms are presented in Table 2. The total porosity of FGM layers varied from 30% to approximately 50%, as controlled by the amount of RS added. It should be noted that 0% RS is not equivalent to zero porosity. The sintering tests of Al_2O_3 powder (in analogous process conditions) with no rice starch addition indicated the presence of some amount of inherent porosity in ceramic structure.

Based on the analysis of the graph of pore size distribution, it can be stated that the volume fraction of the rice starch addition strongly influences on the amount, size, and shape of open pores in the ceramic preform. Figure 7 presents the SEM micrograph of a porous ceramics with a porosity of about 50% (40% RS). Channel pores can be seen in the photographs, with a cross section under 2 µm, distributed uniformly throughout the volume, which makes it possible to infiltrate liquid metal into the preforms.

Figure 8 presents the micrograph of a bridge connecting ceramic αAl_2O_3 grains that was formed during the sintering of the preform. Surface analysis of element distribution (EDS) has shown that properly selected parameters of burning the organic additives have ensured the purity of the chemical composition of the preform.

Based on the performed observations and EDS analysis, taking into account quality analysis, it can be concluded that the connections between the ceramic grains of aluminum oxide have the same chemical composition as their surface.

Fig. 5 Conditions and parameters under which application tests were conducted; three cycles: **a** max 300 s at loads:100 N, 210 N, 316 N, 536 N, 737 N, rotation speed of disc 2000 rpm, duration ~ 50 s; **b** load 300 N, rotation speed of disc 2000 rpm, duration ~ 1800 s, wet lubrication (including 10 water spray events—10 s each); **c** load/speed combinations (2000–4000 rpm, 200–300 N) conditions, duration ~ 600 s, wet lubrication

Mechanical and thermal measurements of ceramics with different amounts of porosity have also been conducted. The values of hardness as well as three-point bending resistance were determined, and tests of heat conductivity as a function of temperature were conducted. The obtained results for preforms with varying shares of pores are presented in Table 3.

The hardness measurement had an error resulting from the lack of a clear impression of the hardness meter's indenter. The lower hardness was characterized by a higher relative measurement error (~ 7%), while for higher hardness, the measurement error was ~ 2%. Hardness tests using the Vickers method provide important data regarding the strength of the porous ceramics and the possibility of its being damaged in reaction to external loads (e.g., during the infiltration with liquid metal). The results of bending resistance of porous ceramic preforms have shown that the lowest resistance of 43 MPa was found for preforms with the highest porosity, i.e., 50% and that this value is approximately 50% lower than the resistance of the preform with porosity ~ 30%. This is an important clue for the selection of technological parameters of the infiltration process. The conducted tests of heat conductivity have confirmed an adverse impact of the porosity on the thermal properties of those materials. The ceramic by itself has a low thermal conductivity (for Al_2O_3 thermal conductivity is about 20–30 W/m•K);
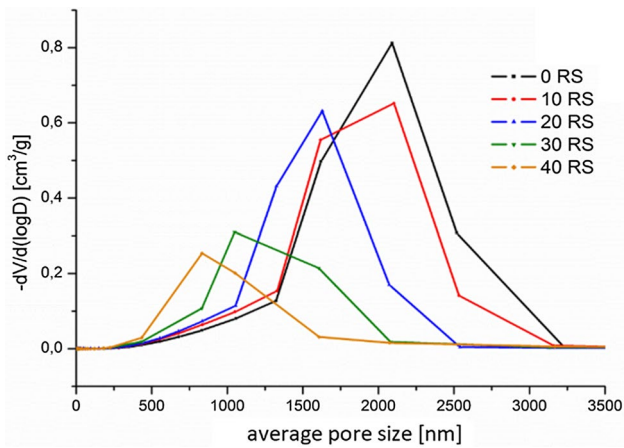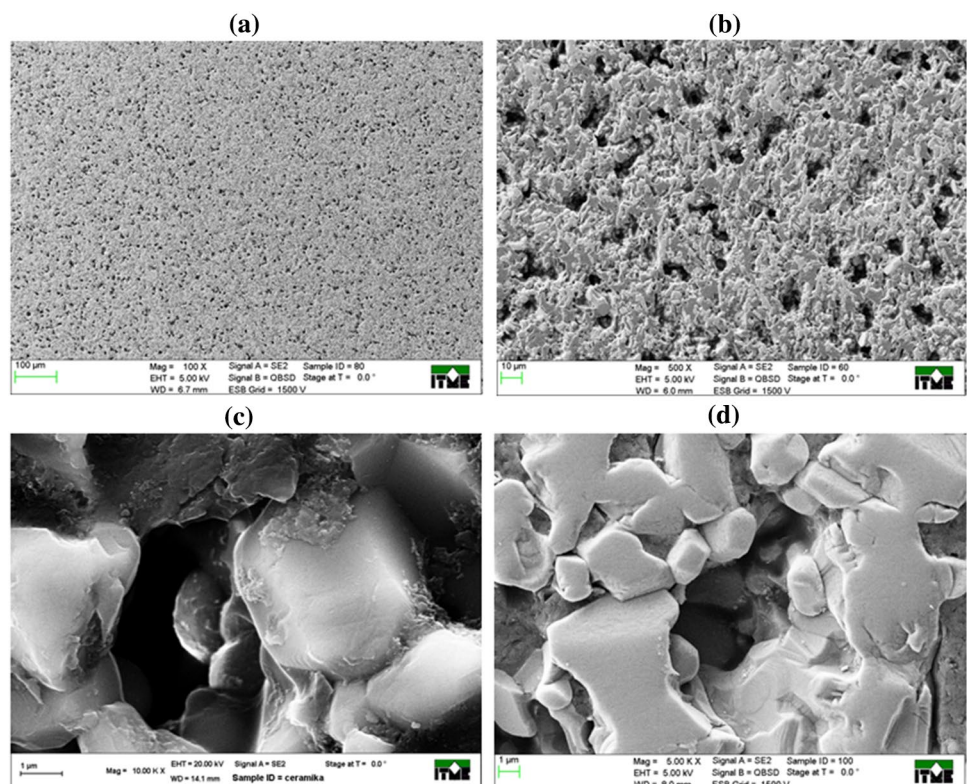
Fig. 6 Pore size distributions of porous ceramic preforms with different amounts of rice starch (RS)

additionally, the presence of pores results in a significant drop in this value. (The pores form a sort of barrier for the heat transfer within the material.)

3.2 Characterization of Cu–Al$_2$O$_3$ composite

Composite materials obtained via infiltration of the porous preforms have undergone characterization. The detailed microstructural observation (by SEM), confirmed by the elements surface distribution (by EDS), has shown the complete filling of porous preforms with copper (Fig. 9). Furthermore, no significant structural defects were observed in the obtained composites, just porosity below approximately 5%, localized to areas within the ceramic phase (enclosed porosity resulting in the stage of preform manufacturing, as well as tear-outs occurring in the material during its machining).
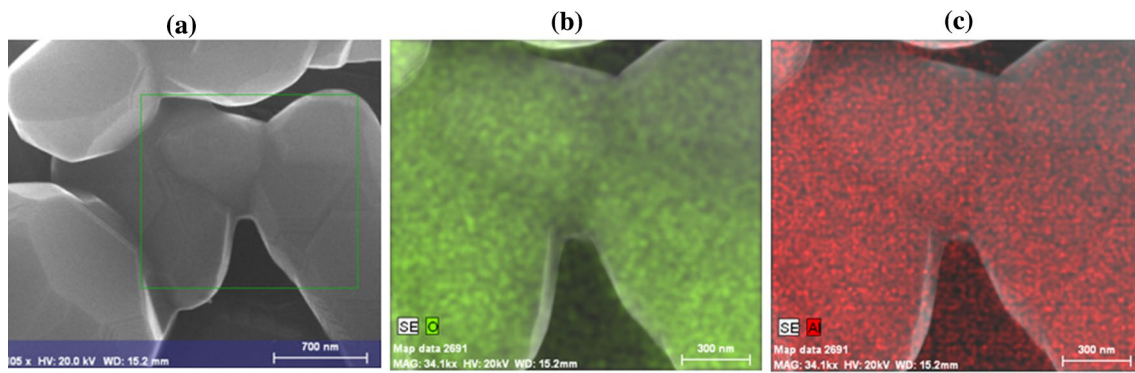
Table 2 Porosity of ceramic preforms measured by mercury porosimetry and by Clemex

Alumina preform	Average size of pores (nm) POROSIMETER	Total porosity (%) POROSIMETER	Open porosity (%) CLEMEX	Closed porosity (%) CLEMEX	Total porosity (%) CLEMEX
0%RS	857.1	**30.0**	25.3	1.4	**26.7**
10%RS	1102.2	**35.5**	31.6	1.2	**32.8**
20%RS	1328.3	**44.2**	39.1	1.8	**40.9**
30%RS	1559.8	**46.1**	43.2	0.8	**44.0**
40%RS	1693.7	**50.0**	45.2	1.1	**46.3**

Bold values indicate total porosity (%) which was included in further research

Fig. 7 SEM micrographs of alumina ceramic preform (40%RS) after sintering; metallographic section of the preform surface **a**–**b**; breakage structure of the preform **c**–**d**

(a)

(b)

(c)

(d)

Fig. 8 SEM micrograph (**a**) and an EDS analysis (**a–b**) of the surface distribution of the elements of the breakage structure of the ceramic preform manufactured out of aluminum oxide

Table 3 Mechanical and thermal properties of porous ceramic preforms

Preform	HardnessHV10	Bending strength (MPa)	Thermal conductivity (W/m·K)				
			50 °C	100 °C	200 °C	400 °C	600 °C
0%RS	310	89.2±5.5	13.3±1.2	11.4±2.1	9.1±2.3	6.3±2.4	4.6±2,8
10%RS	170	75.1±8.5	1.6±1.5	8.9±2.9	7.2±1.8	4.9±2.0	3.7±1.2
20%RS	58	68.4±6.3	9.2±0.8	8.1±1.4	6.5±1.5	4.5±3.1	3.4±26
30%RS	27	50.7±7.5	8.5±2.5	7.6±1.6	6.0±2.0	4.2±2.2	3.0±3.2
40%RS	12	43.2±4.5	8.0±1.8	7.1±2.2	5.8±1.2	4.1±1.2	2.8±3.1

In addition, the conducted microstructural analysis via a scanning microscope does not indicate the occurrence of an intermediate phase between the copper and the aluminum oxide, created after the pressure infiltration process. One of the hypotheses suggested in the literature that has been confirmed in the case of using the copper direct bonding technique is the creation of non-stoichiometric compounds on the boundaries of $Cu–Al_2O_3$ composite grains—aluminum–copper spinels. Observations were also made regarding the possibility of aluminum spinel and copper oxide occurrence within the structure, which significantly impact the thermal and mechanical properties of composites. Even though their presence results in increased hardness and resistance to cracking, on the other hand it substantively lowers the ability to heat dissipation generated via friction. It should be noticed that the most important factors for materials dedicated to brake disc application are good tribological properties and high thermal conductivity. In order to accurately observe the Cu/Al_2O_3 boundary in $Cu–Al_2O_3$ composites, tests were conducted via a transmission electron microscope. The results of those observations are presented in Fig. 10.

TEM tests have confirmed the good bonding of the ceramic phase with the copper matrix, and the observation of the metal/ceramics boundary has shown no occurrence of new components. The conducted pressure infiltration process in an autoclave has ensured an oxygen-less atmosphere, with oxygen being the initiating agent of the formation of spinel compounds within the composite structure.

Subsequently, measurements were conducted of the density and porosity, using the Archimedes method, as well as measurements of the thermal properties of composite materials with a different volume fraction of the aluminum oxide. Table 4 presents the basic properties of $Cu–Al_2O_3$ composite materials after infiltration process with a designed porosity (0%RS—40%RS).

The measured thermal conductivity values of the obtained composites are slightly below the expected values. It is assumed that the thermal conductivity of copper is 396 W/(m·K), sintered Al_2O_3 above 20 W/(m·K); therefore, the obtained results should be within the above-listed boundaries. As the share of the metallic phase increases, an increase in thermal conductivity of composites can be observed, which reaches the value of 179 W/(m·K) for material containing 46% vol. of copper in the composite. The increase in the volume fraction of the Al_2O_3 in the composite causes decrease in the materials thermal conductivity. It is caused by the increase in the value fraction of phase with a lower value of thermal conductivity. For the highest share of aluminum oxide in the composite ($Cu–Al_2O_3$ (0%RS)), the lowest thermal conductivity value was recorded at 107 W/(m·K). The reason why lower thermal conductivity values

Fig. 9 SEM micrograph as well as EDS surface distribution of elements of the $Cu-Al_2O_3$ composite resulting from infiltrating with copper preform with porosity ~ 40%; white—Al, blue—O, red—Cu
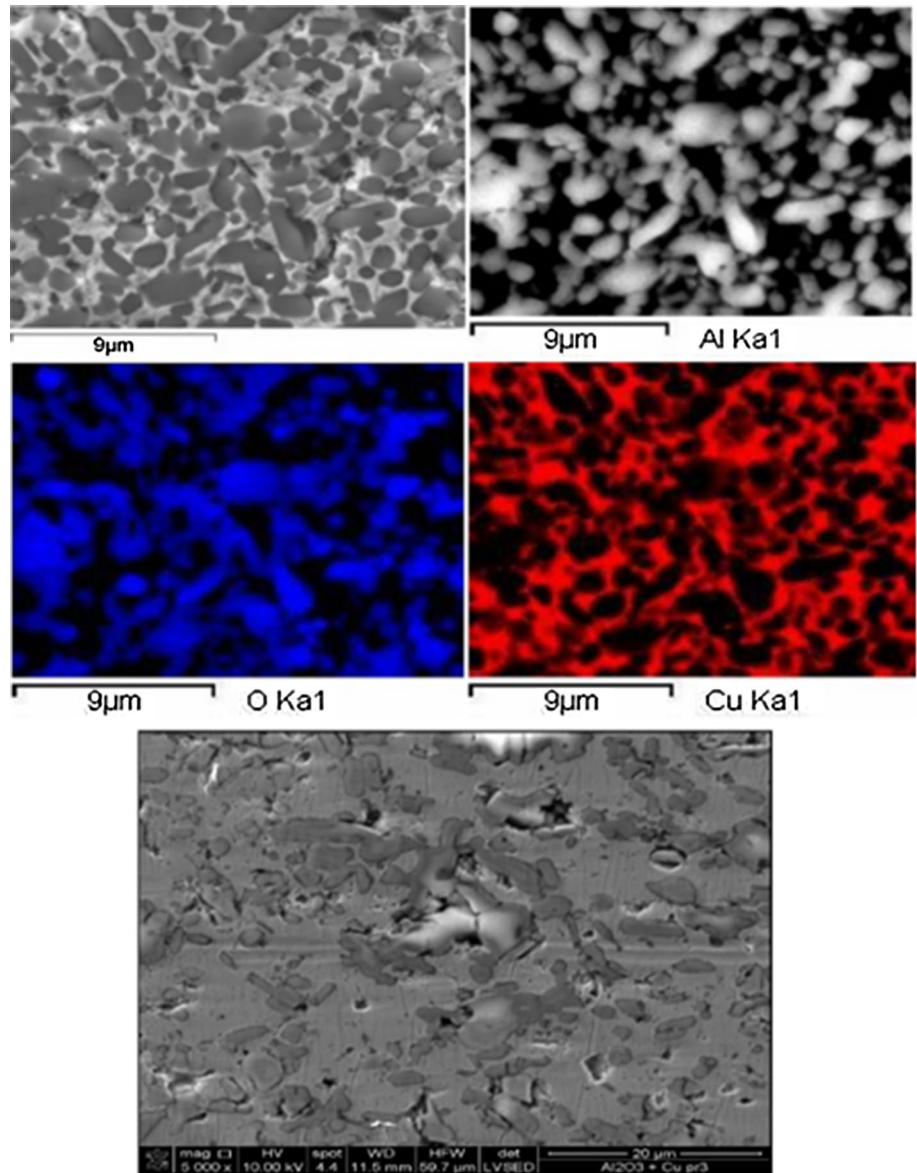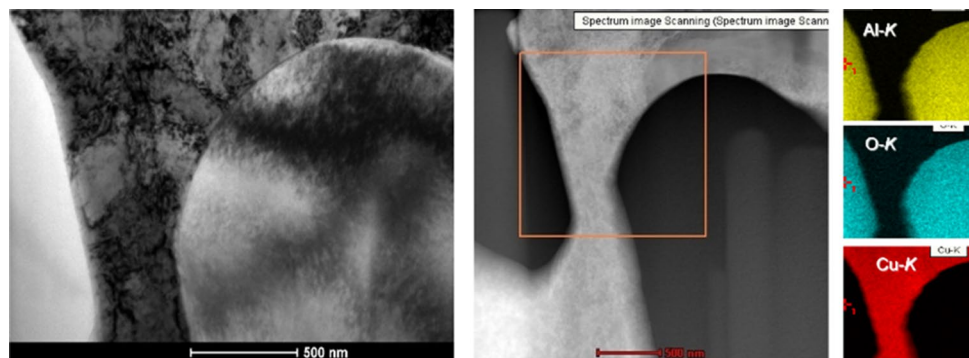

Fig. 10 The microstructure (TEM) of the aluminum oxide–copper grain boundary, as well as quality analysis of elements in the nano-area

occur compared to those expected might be due to the porosity present in the composite structure. The visible lowering of thermal conductivity resulting from porosity is observed in the case of the $Cu-Al_2O_3$ composite (20% RS) (Table 4).

The conducted measurements of the thermal properties have key importance for the possibility of using such materials in heat-dissipating systems.

Table 4 Physical and thermal properties of Cu–Al$_2$O$_3$ composites obtained via infiltration of porous ceramic preforms with varying porosity

Ceramic preform		Composite Cu–Al$_2$O$_3$			
Preform	Porosity (vol.%)	Amount of Cu (vol.%)	Porosity (vol/.%)	Density (g/cm^3)	λ at 50 (W/mK)
0%RS	29.5	26.6	2.9	5.2	107
10%RS	33.0	32.0	1.0	5.5	121
20%RS	41.7	39.1	2.6	5.6	144
30%RS	44.4	39.5	4.9	5.6	140
40%RS	48.9	45.7	3.2	6.1	179

3.3 Application tests

The prepared demonstrators of disc brakes (gradient (FGMD) as well as un-gradient) underwent wear resistance tests for varying conditions of the friction process. For reference materials, discs were used that were manufactured out of grey iron, currently used as braking discs (CID). Prior to the tribological tests, the demonstrators were examined to determine the quality of their surfaces. The surface roughness parameter R_a was determined (average arithmetic deviation of the profile). As shown in Fig. 11, the highest roughness parameter was found for the demonstrator that was a gradient material (FGMD), but the differences were not significant.

Tests of abrasive wear of the demonstrators of brake discs were conducted in various friction cycles. In the first work cycle of the demonstrators of brake discs, varying loads were assumed, with a constant rotation speed of the disc at 2000 rpm, in dry lubrication conditions. The friction coefficient measurement results and the temperature changes of the surface of tested disc demonstrators for the selected values of the loads used are presented in Figs. 12, 13.

For the lowest value of load (100 N), the friction coefficient of FGMD sample was 0.25, stable in whole time of test and similar to the literature data [20]. During the test, which used the load of 316 N, the composite disc (UD) was destroyed after approximately 180 s. During the friction, an increase in temperature of the disc was recorded up to approximately 250 °C, after which the disc cracked, which led to its exclusion from further research. For other two materials tested (FGMD and CID), the obtained values of CoF were similar.

Fig. 11 Graphical illustration of the roughness profiles of the surfaces of the studied demonstrators, with the determination of the amplitude parameter of roughness Ra; **a** Ra (CID) = 0.53 μm, **b** Ra (FGMD) = 1.20 μm, **c** Ra (UD) = 0.37 μm

(a)
(CID) Ra = 0.53 μm

(b)
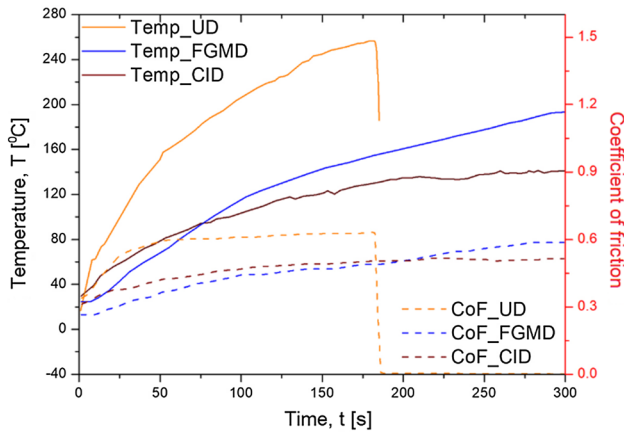**(FGMD) Ra = 1.20 μm**

(c)
(UD) Ra = 0.37 μm

Fig. 12 The course of the coefficient of friction (CoF) as well as temperature as a function of time of the dry friction process for the load of 316 N
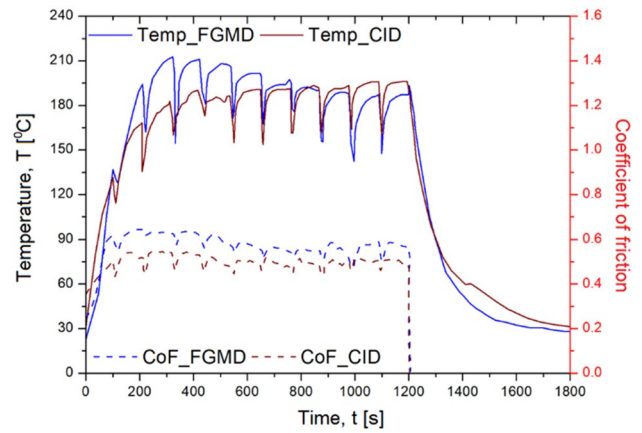

Fig. 14 The course of the coefficient of friction (CoF) as well as temperature as a function of the time of the wet friction process (cyclical administering of the lubricating agent every 10 s)
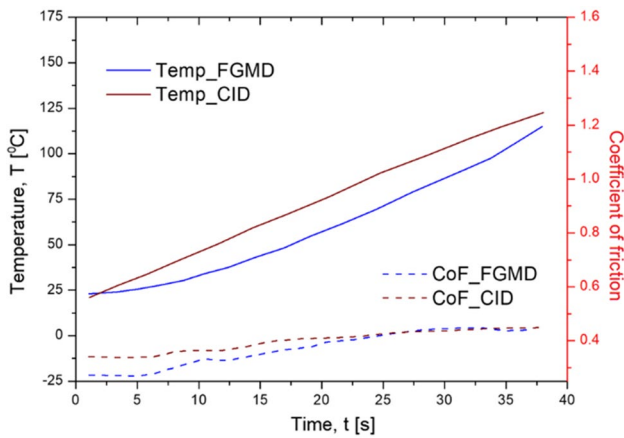

Fig. 13 The course of the coefficient of friction (CoF) as well as temperature as a function of time of the dry friction process for the load of 737 N

Fig. 15 The course of the coefficient of friction (CoF) as well as temperature as a function of time of the dry friction process

For the highest value of load used (737 N), in the dry lubrication cycle, the disc manufactured out of a gradient material (FGMD) had a similar temperature and friction coefficient value compared to the disc manufactured of grey iron (CID). It can be concluded that such a graded structure gives a promising results both from friction and from thermal properties.

In the next stage of tribological research, friction tests were conducted in the conditions of wet lubrication. For the lubricant, water was used, administered to the contact area cyclically every 10 s. In Fig. 14, selected results of the friction coefficient and the temperature changes of the tested brake disc demonstrators tested in wet lubrication conditions are presented.
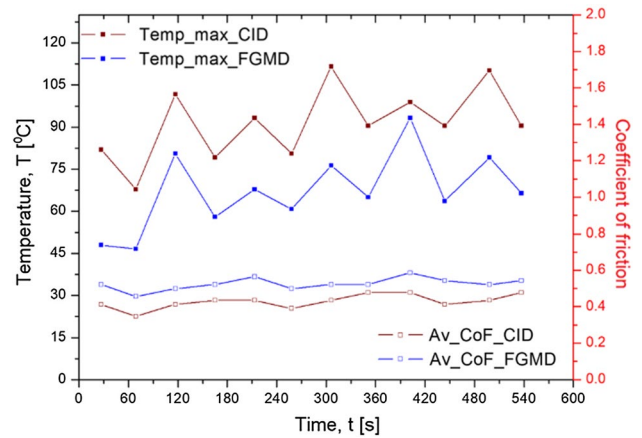
In the wet lubrication conditions, both discs, i.e., FGMD and CID, had a stable course of temperature as a function of time and had similar friction coefficient values. The subsequent friction test was conducted in dry lubrication conditions with a variable rotation speed, i.e., 2000–4000 rpm, and a variable load 200–300 N. The obtained results are presented in Fig. 15. The assumed work cycle in the case of using changing loads loosely approximated the actual conditions of work of a break disc of a car moving in an urban environment.

When analyzing the obtained results, one may note that the demonstrator of a brake disc manufactured of a gradient material had the best dissipation properties for the heat generated in the system. Additionally, it had a similar value of the coefficient of friction to the demonstrator serving as a reference material.

Comparing the obtained friction coefficient results with reference to the literature data, it can be stated that they are at a similar level to the results presented in [21]. The literature value of the friction coefficient for pure copper is 0.53 [22]. Depending on the type of reinforcement phase, its quantity and form, as well as the counter-sample material and friction process conditions, it may oscillate around this value. With the increase in materials hardness, which is caused by a high amount of ceramic phase, resistance of movement is raising and thus increase in the friction coefficient is observed. The outer layer in the gradient disk that was subjected to friction tests contained about 45% of the ceramic phase, so the obtained values of the friction coefficient for the tested material were 0.3–0.45 in wide range of tested loads. In the article [23] where the tribological properties of material based on copper (56% wt.) and iron (18% wt.) doped with SiC (2% wt.) and graphite (6% wt.) were tested, the measured value of the friction coefficient was 0.4 and the authors suggest that this is a very good value for the use of this material in the braking system. The authors of [24] examined material very similar in composition and obtained a friction coefficient value between 0.45 and 0.65. In our case under constant speed and increasing load conditions, a slight increase in the friction coefficient of the gradient disk was observed from about 0.30 (at 100 N load) to 0.45 (at 737 N load). This statement is in good agreement with results of [22]. They stated that friction and deformation occur mainly on the copper matrix because the softening effect of copper is caused by high temperature on the surface. As an effect of friction, the wear products of copper are easy to transfer onto counter-body and friction relationship transforms from early copper–iron steel into copper–copper friction process. The temperature plays a significant role in the friction process and generates high level of residual stresses. Weaker heat dissipation in the case of a non-gradient disk was the reason for its cracking in the initial testing phase.

The introducing of a cooling lubricant during tests resulted in the friction coefficient varying within the range between 0.5 and 0.6. Its behavior is quite similar to the reference cast iron disc. The friction process in the wet condition was not stable. The dynamic changes in the materials behavior can be seen. High temperature of the surface and presence of water can provide the surface oxidation of copper and increase in friction resistance. The raise in the coefficient of friction can be attributed to the oxide layer formed during manufacturing process on the surface of samples and is associated with the increase in surface temperature due to friction process [23].

From a practical point of view, the most valuable are the results of tests obtained in the so-called urban driving mode (at variable speed and load). Comparing the obtained friction coefficient results of the gradient disk with the cast iron reference material, its low and stable value should be emphasized. In the analyzed period of the test, the value of the friction coefficient ranged between 0.5 and 0.6 and only slightly exceeded the analogous value for the cast iron disk. Additionally, it was found that the gradient disc was effective in dissipation of heat.
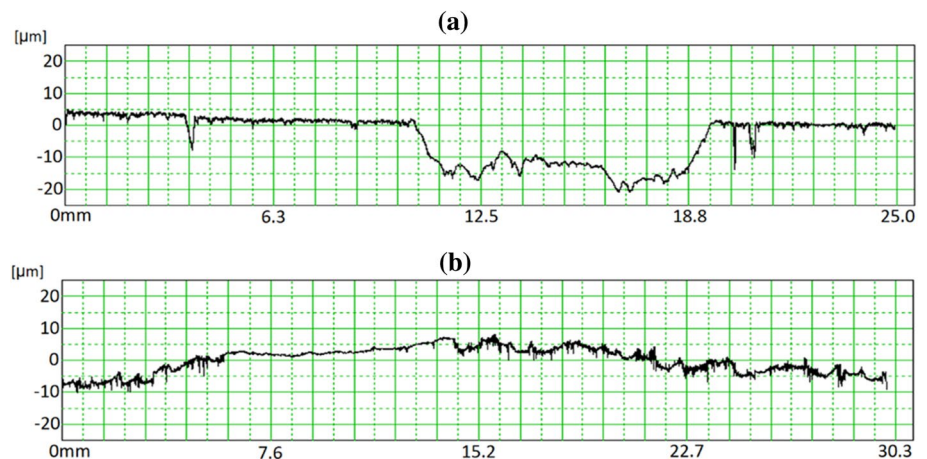
Disc demonstrators after the friction tests underwent wear assessment. Profilometric measurements were made of the depth of the groove resulting from the tests (Fig. 16). The appearance of the discs after the tests is presented in the photograph (Fig. 17).

The representative microstructure of the surface area after wear tests is presented in Fig. 18.

As we observed, the microstructure of the FGMD disc surface of the grooves is very homogeneous and relatively smooth.

There was a plastic deformation/abrasion consisting in covering the ceramic phase with plastic copper. Slip lines are visible along which the counter-body had travelled. This is abrasive wear based on plastic deformation. No visible loose wear products are pressed into the groove surface during the wear process.

Fig. 16 Profilometers of the wear of the groove in demonstrators of brake discs created after the friction tests; **a** CID and **b** FGMD
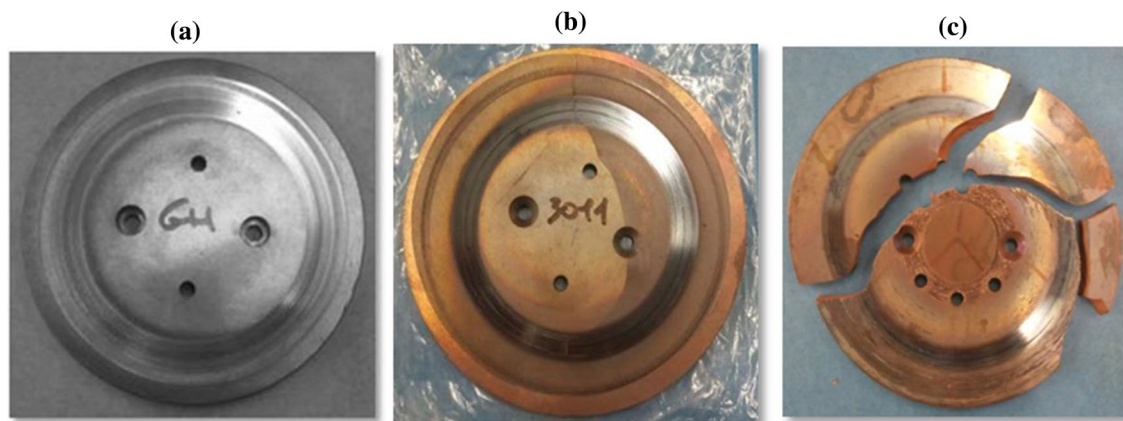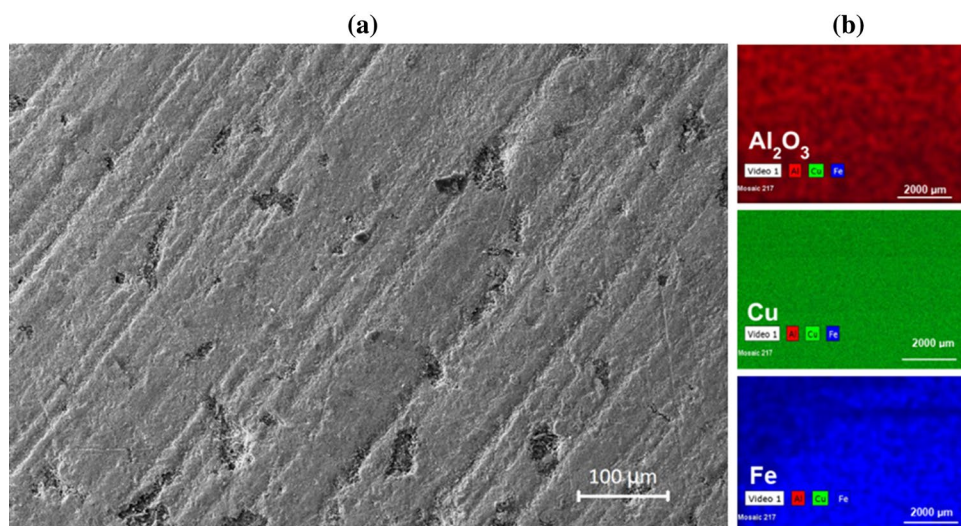
Fig. 17 Disc demonstrators after application tests; **a** CID—iron disc, **b** FGMD—gradient disc, and **c** UD—composite disc

Fig. 18 The microstructure (**a**) and quality analysis of elements (**b**) of the FGMD material surface after wear tests

It was determined that the demonstrator manufactured of a gradient material FGMD was not worn out after the conducted friction tests. Only a slight smoothing of the surface was observed in the area of working against a counter-sample. The brake disc manufactured of iron (reference material) underwent some wear, and the depth of the resulting groove was approximately 20 μm (Fig. 18a). It can therefore be concluded that the life span of the disc with a composition gradient should be higher, compared to the discs in use today.

4 Conclusion

The latest literature reports show great interest in the use of metal matrix composites for use in brake systems in high-speed trains. These materials can typically withstand higher temperatures and can be used to temperatures over 1000 °C. Particularly, copper matrix composites are the top choices

as brake materials for cars and high-speed trains due to their attractive properties such as high thermal conductivity, excellent tribological properties, and adaptability to working conditions [20–23]. The presented results are in line with the global trend of research on multiphase materials. Based on the obtained results, it can be concluded that:

- rice starch as a porous agent ensures open porosity in ceramic preforms with a wide porosity range (from 30 to 50% by volume),
- pressure infiltration allows for obtaining graded materials based on porous ceramic preform without any discontinuities or microcracks,
- good bonding at metal/ceramics interface was obtained with no other phases identified after the infiltration process,
- specially designed graded structure of the Cu–Al$_2$O$_3$ demonstrator disc ensures high hardness of the contact

surface (due to the high ceramic content), and effective heat dissipation through the volume of material (due to the high thermal conductivity of copper),

- on the one hand, the structure ensures high hardness of the contact surface, and effective heat dissipation,
- the level of friction wear is lower in comparison with gray iron disc, which proves the high application potential of the developed materials.

Compliance with ethical standards

Conflict of interest The authors declare that they have no conflict of interest.

Ethical approval The article was prepared according to the rules of good practice.

References

1. Miracle DB. Metal matrix composites—From science to technological significance. Compos Sci Technol. 2005;65:2526–40.
2. Nicholls CJ, Boswell B, Davies IJ, Islam MN. Review of machining metal matrix composites. Int J Adv Manuf Technol. 2017;90:2429–41.
3. Scherm F, Völkl R, Neubrand A, Bosbach F, Glatzel U. Mechanical characterization of interpenetrating network metal–ceramic composites. Mat Sci Eng A. 2010;527:1260–5.
4. Wannasin J, Flemings MC. Metal matrix composites: infiltration. Wiley Encycl Compos. 2012;3:1747–9.
5. Jhaver R, Tippur H. Processing, compression response and finite element modeling of syntactic foam based interpenetrating phase composite (IPC). Mat Sci Eng A. 2009;499:507–17.
6. Panda S, Dash K, Ray BC. Processing and properties of Cu based micro- and nano–composites. B Mater Sci. 2014;37:227–38.
7. Fathy A, El-Kady O. Thermal expansion and thermal conductivity characteristics of Cu–Al$_2$O$_3$ nanocomposites. Mater Des. 2013;46:355–9.
8. Sobczak J, Drenchev L. Metallic functionally graded materials: a specific class of advanced composites. J Mater Sci Technol. 2013;29:297–316.
9. Maj J, Basista M, Węglewski W, Bochenek K, Strojny-Nędza A, Naplocha K, Panzner T, Tatarková M, Fiori F. Effect of microstructure on mechanical properties and residual stresses in interpenetrating aluminum-alumina composites fabricated by squeeze. Mater Sci Eng A. 2018;715:154–62.
10. Gasik MM. Functionally graded materials: bulk processing techniques. Inter J Mater Prod Tec. 2010;39:20–9.
11. Winzer J, Weiler L, Pouquet J, Roder J. Wear behavior of interpenetration alumina-copper composites. Wear. 2011;271:2845–51.
12. R. Mahamood, E. Akinlabi, Functionally Graded Materials: An Overview, Proceeding of the World Congress on Engineering 4–6 (2012) London, 3
13. Muller E, Drasar C, Schilz J, Kaysser WA. Functional graded materials for sensor and energy applications. Mater Sci Eng A. 2003;362:17–39.
14. Konopka K, Oziębło A. Microstructure and the fracture toughness of the Al$_2$O$_3$–Fe composites. Mater Charact. 2001;46:125–9.
15. Moon RJ, Hoffman M, Rödel J, Tochino S, Pezzotti G. Evaluation of crack-tip stress field on microstructural-scale fracture in Al–Al$_2$O$_3$ interpenetrating network composites. Acta Mater. 2009;57:570–81.
16. Chmielewski T, Golański D, Włosiński W. Metallization of ceramic materials based on the kinetic energy of detonation waves. Bull Pol Acad Sci-Tech Sci. 2015;63:449–56.
17. Hsu HP, Huang MC. Percolation thresholds, critical exponents, and scaling functions on planar random lattices and their duals. Phys Rev E. 1999;60:6361–70.
18. Herega A. Some applications of the percolation theory: brief review of the century beginning. J Mat Sci Eng A. 2015;5:409–14.
19. Tu JP, Yang YZ, Wang LY, Ma XC, Zhang XB. Tribological properties of carbon-nanotube-reinforced copper composites. Tribol Lett. 2001;10:225–8.
20. Xiao Y, Zhang Z, Yao P, Fan K, Zhou H, Gong T, Zhao L, Deng M. Mechanical and tribological behaviors of copper metal matrix composites for brake pads used in high-speed trains. Tribol Inter. 2019;119:585–92.
21. Sadoun AM, Fathy A. Experimental study on tribological properties of Cu–Al$_2$O$_3$ nanocomposite hybridized by graphene nanoplatelets. Ceram Int. 2019;45:24784–92.
22. Zhang P, Zhang L, Wei D, Wu P, Cao J, Shijia C, Qu X. A high-performance copper-based brake pad for high-speed railway trains and its surface substance evolution and wear mechanism at high temperature. Wear. 2020;444–445:203182.
23. Su L, Ga F, Han X, Chen J. Effect of copper powder third body on tribological property of copper-based friction materials. Tribol Inter. 2015;90:420–5.
24. Purohit R, Kumar Solanki N, Bajpayee G, Rana RS, Hemath Kumar G, Nateria R. Development of Cu–Al2O3–CBN hybrid composite through powder process and analysis of mechanical properties. Mater Today Proc. 2017;4:3270–9.